Pulmonary hypertension after pneumonectomy: a preclinical model in rats and human pulmonary endothelial cells

Pierre Sentenac, Gianluca Samarani, Patrice Bideaux, Pierre Sicard, Benjamin Bourdois, Sylvain Richard, Pascal Colson, Saadia Eddahibi

Pulmonary hypertension after pneumonectomy: a preclinical model in rats and human pulmonary endothelial cells

Pierre Sentenac [a,b,*], Gianluca Samarani[a,b], Patrice Bideaux[a], Pierre Sicard [a], Benjamin Bourdois[a,b], Sylvain Richard[a], Pascal H. Colson [b] and Saadia Eddahibi[a,†]

[a] PhyMedExp, University of Montpellier, INSERM, CNRS, Montpellier, France
[b] Department of Anaesthesiology and Critical Care Medicine, Heart and Lung Center, Arnaud de Villeneuve Teaching Hospital, Montpellier University School of Medicine, Montpellier, France

* Corresponding author. Département d'Anesthésie Réanimation, Hôpital Arnaud de Villeneuve, Pôle Coeur-Poumons, 371 Avenue du Doyen Gaston Giraud, 34295 Montpellier Cedex 05, France. Tel: +33-788-014-609; e-mail: dr.sentenac@gmail.com (P. Sentenac).

Key question

What are the consequences of pneumonectomy for cardiopulmonary function in rats and the involved mechanisms in vitro?

Key finding(s)

Pulmonary hypertension (PH) and right heart remodelling are related to excessive muscularization of distal pulmonary arteries.

Take-home message

The shear stress related to high blood flow alters the pulmonary endothelial paracrine control of smooth muscle cell growth, leading to PH.

Pathophysiology of the post-pneumonectomy syndrome. Main mechanisms leading to pulmonary hypertension and heart disease after pneumonectomy.

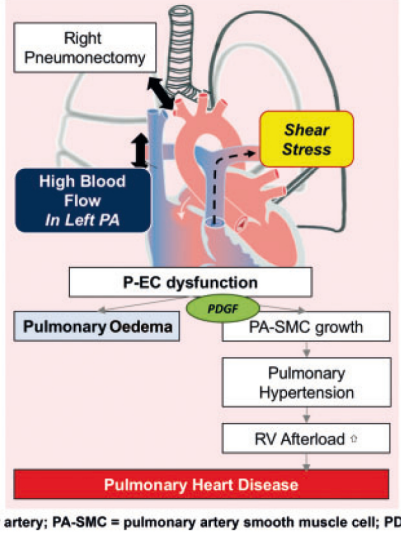

PA = pulmonary artery; PA-SMC = pulmonary artery smooth muscle cell; PDGF = Platelet-derived growth factor; P-EC = pulmonary endothelial cell; RV = right ventricle

Abstract

OBJECTIVES: Pulmonary hypertension and heart disease contribute to the high morbidity rate following pneumonectomy (PN). The pathophysiology is still poorly understood. The objective was to investigate the consequences of PN on cardiopulmonary function in rats and to explore *in vitro* the involved mechanisms.

METHODS: Sixty Sprague-Dawley male rats randomly underwent either a right PN (PN group) or sham surgery. Ten rats per group were sacrificed on postoperative days 3, 7 and 28. Cardiopulmonary alterations were investigated by echocardiographic, haemodynamic and histological analyses. *In vitro*, the shear stress was reproduced using a Flexcell Tension™ cyclic stretch on cultured human pulmonary

[†] Deceased.

Presented at the 33rd Annual European Association of Cardiothoracic Anaesthesiology (EACTA) Congress 2018 in Collaboration with ACTACC, Manchester, UK, 19–21 September 2018, first prize in the category 'best oral presentation'.

endothelial cells (P-ECs) to investigate the impact on pulmonary artery smooth muscle cell (PA-SMC) growth. Data are expressed as mean ± SD.

RESULTS: Mean pulmonary arterial pressure gradually increased in the PN group to reach 35 ± 7 mmHg on postoperative day 28 vs 18 ± 4 in sham ($P = 0.001$), likewise the proportion of muscularized distal pulmonary arteries, 83 ± 1% vs 5 ± 1%, respectively ($P < 0.001$), related to *in situ* PA-SMC proliferation. The right ventricle area and lateral wall thickness were doubled in the PN group on postoperative day 28. The left ventricle ejection fraction decreased on postoperative days 7 and 28 while the right ventricle function was maintained. *In vitro*, the human PA-SMC growth was significantly greater when seeded with stretched vs non-stretched P-EC media, highlighting the role of shear stress on the P-EC paracrine function.

CONCLUSIONS: Right PN led to pulmonary hypertension and proportional right heart remodelling in rats. The shear stress related to high blood flow alters the pulmonary endothelial paracrine control of SMC growth..

Keywords: Pneumonectomy • Pulmonary hypertension • Pulmonary heart disease • Models • Animal • Endothelial cells • Growth factors

ABBREVIATIONS

ANOVA	Analysis of variance
COPD	Chronic obstructive pulmonary disease
LV	Left ventricle
mRNA	Messenger ribonucleic acid
MTT	3-(4,5-dimethylthiazol-2-yl)-2,5-diphenyl tetrazolium bromide
P-EC(s)	Pulmonary endothelial cell(s)
PA-SMC(s)	Pulmonary artery smooth muscle cell(s)
PAP	Pulmonary arterial pressure
PDGF	Platelet-derived growth factor
PH	Pulmonary hypertension
PN	Pneumonectomy
RV	Right ventricle
WHO	World Health Organization

INTRODUCTION

Surgery serves a major role in lung cancer management, but large pulmonary resections are still associated with elevated postoperative morbidity rate [1]. Right pneumonectomy (PN) is associated with the poorest outcome [2, 3]. Pulmonary hypertension (PH) is a frequent complication following PN [4] that could contribute to decrease the postoperative quality of life [2] and survival [4, 5]. PH could lead to heart dysfunction [6, 7], supraventricular tachyarrhythmia [7, 8] and pulmonary oedema [9]. Although described in literature, the pathophysiology of PH in the context of PN is unique, poorly investigated and not explicitly mentioned in the 2019 updated WHO classification [10].

Despite several studies in the field of pulmonary resection surgeries, the results are discordant and have some limitations. Most studies were performed in small cohorts of large animals [11–13]. In the few studies carried out in rats, PN was frequently combined with monocrotaline [14, 15], or another additional hit [16], in multiple-hit models, which is less directly relevant to the scope of thoracic surgery.

Increased blood flow in the remaining pulmonary arteries is suspected to play a key role in the development of PH after PN. The role of disturbed blood flow is well recognized in other PH diseases. Aorto-pulmonary or aorto-caval shunt surgeries, well-known models of congenital heart disease [17], expose the pulmonary vascular bed to excessive blood flow. This appears to activate several signalling pathways that promote pulmonary arteriolar vasoconstriction, inflammation and thickening, leading to PH.

After PN, halving the pulmonary vascular bed automatically leads to high blood flow in the remaining lung. The shear stress represents the mechanical forces resulting from the flow rate and velocity of the surrounding fluid across the surface of vessels. It is clearly established that the pulmonary endothelial cells (P-ECs) convert mechanical signals into biochemical signals affecting pulmonary vascular tone, permeability and remodelling [17], in human and experimental PH [18]. Our hypothesis is that the P-EC function is altered by increased blood flow in the contralateral lung after PN, leading to pulmonary artery smooth muscle cell (PA-SMC) growth and PH development.

The aim of the present study was to comprehensively investigate the consequences of right PN on pulmonary circulation and heart function *in vivo* in a rat model. Primary outcome was invasive pulmonary arterial pressure (PAP). Pulmonary artery muscularization and remodelling were described. Heart function and pulmonary oedema were also studied. As PN is associated with increased blood flow in the remaining lung, we sought to determine *in vitro* the effects of a pathological cyclic stretch exposure on the phenotype of cultured human P-ECs and PA-SMCs.

MATERIALS AND METHODS

In vivo study

All experiments were conducted in the PhyMedExp laboratory, according to the 'Guide for the Care and Use of Laboratory Animals', also in compliance with the 'NC3Rs ARRIVE' guidelines. The protocol was approved by an Ethics Committee (No 3775) and authorized by the French Ministry of Education, Research and Innovation (No 2016012514021222).

Sixty adult male Sprague-Dawley rats aged 11 weeks (390 g) were randomized into 2 groups to receive either a right PN (PN group) or a right thoracotomy without pulmonary resection (sham group). The anaesthetic protocol is detailed in the Methods. Ten rats per group were sacrificed on postoperative days 3, 7 and 28 (D3, D7 and D28, respectively).

A standardized transthoracic echocardiography was performed under spontaneous ventilation in isoflurane-anaesthetized rats by the same technician, blinded to the surgery, using a high-resolution small-animal ultrasound machine (Vevo 2100™, FUJIFILM VisualSonics®, Toronto, ON, Canada) at baseline, D3, D7 and D28 if appropriate

At the end of follow-up, mean PAP, right ventricle systolic pressure and systemic arterial pressure were measured by closed-chest catheterization as described previously [19], in ventilated rats. Data acquisition used LabChart7™ (ADInstruments®, Sydney, NSW, Australia).

At the end of catheterization, a complementary lethal dose of barbiturate was administered. Then, the heart was dissected and weighed for the calculation of the right ventricle(RV) hypertrophy index {Fulton index = RV/[left ventricle(LV) + septum] weight} and ventricle-normalized weight [RV or (LV + septum) weight/animal weight]. Then, the RV was fixed in a formalin buffer. Pulmonary oedema was assessed using the wet/dry ratio.

In situ study

The left lung was fixed in the distended state within intratracheal infusion of a formalin buffer. After paraffin embedding, the 5-µm-thick lung and RV sections were mounted on Superfrost™ slides for morphometric and immunohistological analyses. All stainings were analysed with an epifluorescence microscope and NIS-Elements™ software (Nikon® 80i, Tokyo, Japan).

The evaluation of distal artery muscularization was performed as described previously [19]. Briefly, in each rat, 60 intra-acinar arteries (100 µm on average) were examined and categorized as non-muscularized, partially muscularized or muscularized. The relative wall thickness index was also calculated [(external diameter – internal diameter)/external diameter, expressed in %].

PA-SMC proliferation was assessed using a proliferating cell nuclear antigen immunostaining of lung sections from rats on D28, as described previously [20]. The inflammatory process was estimated using the CD68 immunostaining. Nuclei were stained with diamidino-2-phenylindole.

Masson's trichrome staining was performed on RV sections, and the RV fibrosis was quantified (RV fibrosis/RV area).

In vitro study

To investigate the cellular changes in response to increased blood flow, human-cultured P-ECs and PA-SMCs from 10 patients were prepared as previously described [18, 20]. We used lung specimens previously obtained during resection procedures for patients with localized lung cancer, free from PH or COPD, collected at a distance from tumour foci (see patient characteristics in Supplementary Material, Table S1). Written informed consent was obtained from all patients prior to experimentation. The protocol was previously approved by the local ethics committee (ID RCB 2008-A00485-50).

Seeded P-ECs ($10.^5$ cells per well) were serum-starved and exposed over 24 h to high magnitude cyclic stretch elongation, 18% (pathological strain) or 5% (physiological strain) at 1 Hz in an FX-5000 Tension Plus™ system (Flexcell®, Burlington, VT, USA), as described by Birukov *et al.* [21]. Then, the P-EC supernatant was collected and added to seeded PA-SMCs ($10.^5$ cells per well), exposed or not to pathological cyclic stretch for 24 h more (Supplementary Material, Fig. S1). PA-SMC proliferation was also assessed under control media, 0% and 5% foetal calf serum (minimal and maximal proliferation capacity, respectively). At the end of the exposure period, the cell proliferation was measured using tetrazolium salt (MTT) assay. The experiments were performed on 10 samples, and each sample was analysed in triplicate.

A molecular characterization of messenger ribonucleic acid (mRNA) expressed by P-ECs was performed by quantitative reverse transcription-polymerase chain reaction as described previously [18]

Statistical analysis

The primary outcome was mean PAP. Six rats per group were necessary to highlight a difference of mean PAP of 10 mmHg between the sham and PN groups on D28 (expected values 25 and 35 mmHg, respectively, SD = 5 mmHg), with a statistical power of 0.90 and a two-tailed alpha risk of 0.05. The number of rats was increased to 10 rats per group per time point to minimize the risk of type II error. Statistical analysis used Prism 8™ (GraphPad® software, La Jolla, CA, USA). Outliers were analysed, and no action was necessary. All data are expressed as mean ± SD (with median and 'min to max' in box plots). The normality of distribution was assessed using Shapiro–Wilk tests, and heteroscedasticity was assessed using Spearman's test. Two-way ANOVA tests were performed, the 2 factors were the group and time point. *Post hoc* comparisons were performed with the correction of Sidak for multiple comparisons. All *P*-values <0.05 were considered statistically significant.

RESULTS

In vivo study

The perioperative mortality was <10% in the PN group ($n = 3$), all with a haemothorax developed within the first 24 h. Ten rats per group per time point were finally evaluated. There were no missing data among survivors.

Compared to the sham group, the mean PAP was increased on D3, D7 and D28 in the PN group, respectively, 29 ± 8 vs 18 ± 2 ($P = 0.033$), 33 ± 4 vs 19 ± 2 ($P = 0.003$) and 35 ± 7 vs 18 ± 4 mmHg ($P = 0.001$). The right ventricle systolic pressure coherently showed the same evolution (Fig. 1). No significant changes were detected in systemic arterial pressure, right atrium pressure and heart rate.

The RV dilated at the expense of the LV in the PN group, so that the RV/LV ratio was >1 on D28 (1.2 ± 0.3 vs 0.5 ± 0.2 in the sham group, $P < 0.001$) (Fig. 2A) and a paradoxical septum motion occurred (Videos 1 and 2). The RV lateral wall thickness approximately doubled in the PN group on D28 compared to the sham group, 1.8 ± 0.3 vs 0.9 ± 0.2 mm ($P < 0.001$), close to the thickness of the LV anterior wall (Fig. 2B). The RV fractional area change was preserved in both groups, while the LV ejection fraction decreased in the PN group on D7 and D28, respectively, 66 ± 13 vs 74 ± 7% ($P = 0.025$) and 65 ± 7 vs 78 ± 6% ($P = 0.007$) (Fig. 2C). Besides, the RV outflow tract cardiac output remained comparable between groups over time

In the PN group, the RV hypertrophy was confirmed by both the RV hypertrophy index and RV-normalized weight (Fig. 3). The LV-normalized weight remained comparable in both groups. Animal weight was comparable in both groups on D28

The lung wet/dry ratio increased on D3 from 4.9 ± 0.2 in the sham group to 5.5 ± 0.4 in the PN group ($P < 0.001$). This difference was no longer observed on D7 and D28 (Fig. 3C).

In situ study

Compared to the sham group, the proportion of muscularized distal pulmonary arteries was increased in the PN group on D7 and D28, respectively 67 ± 2% vs 5 ± 1% ($P < 0.001$) and 83 ± 2% vs 5 ± 1% ($P < 0.001$) (Fig. 4). In addition, the relative wall thickness index of muscularized arteries increased markedly in the PN group on D7 and D28 (Fig. 5A). Some pseudo-occluded distal pulmonary arteries were detected in the PN group on D28 (Fig. 5B).

In line with the muscularization, the proliferating cell nuclear antigen staining showed an abnormal *in situ* PA-SMC proliferation in the PN group (Fig. 6A), and more macrophage infiltrate at the alveolar and perivascular levels (Fig. 6B). The fibrosis deposits were more important in the RV sections of PN rats on D7 and D28

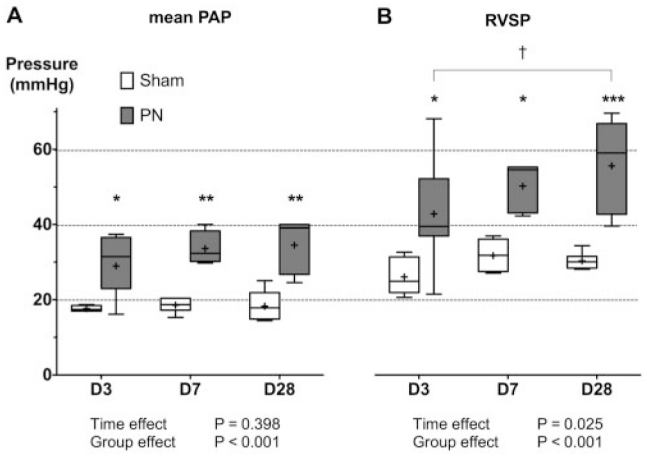

Figure 1: Haemodynamic assessment of pulmonary hypertension. Mean PAP (**A**) and RVSP (**B**) measured by right heart catheterization in the sham and PN groups on D3, D7 and D28 (mean ± SD, median, min to max). Two-way ANOVA tests with Sidak correction: adjusted *P*-values (*) <0.05, (**) <0.01 and (***) <0.001 for comparing sham vs PN at each time point; adjusted *P*-values (†) <0.05, (††) <0.01 and (†††) < 0.001 for comparing time effect in each group. D3: postoperative day 3; D7: postoperative day 7; D28: postoperative day 28; PAP: pulmonary arterial pressure; PN: pneumonectomy; RVSP: right ventricle systolic pressure.

In vitro study

The human PA-SMC proliferation was significantly greater when incubated with stretched P-EC media than non-stretched P-EC media (Fig. 7). However, the exposure of cultured human PA-SMCs to a pathological stretch did not affect PA-SMC growth, highlighting that human P-ECs were more reactive to the magnitude of cyclic stretch than PA-SMCs.

As compared to mRNA level in non-stretched P-ECs, the platelet-derived growth factor (PDGF) mRNA was twice as high as in stretched P-ECs, while basic fibroblast growth factor and epidermal growth factor remained unchanged. Concerning the explored vascular tone pathways, the endothelial nitric oxide synthase seemed to be overexpressed whereas the endothelin-1 did not change

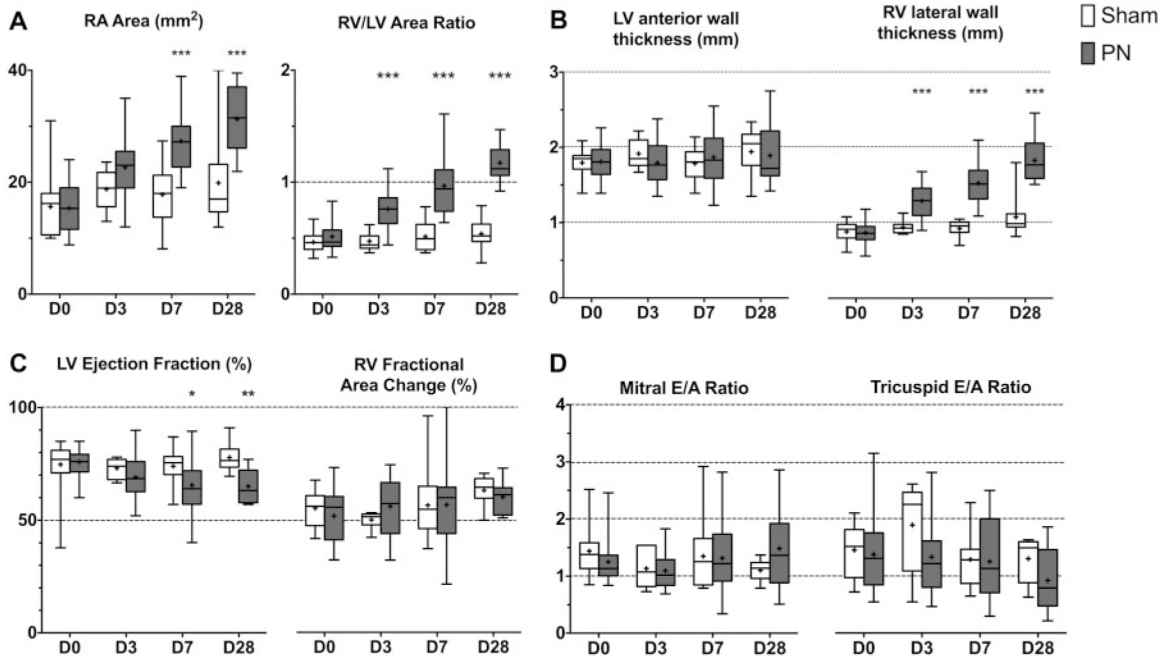

Figure 2: Echocardiographic follow-up. Echocardiographic measurements in the sham and PN groups on D0, D3, D7 and D28 (mean ± SD, median, min to max): (**A**) RA area and RV/LV area ratio measured in the apical four-chamber view; (**B**) end-diastolic LV anterior wall thickness and RV lateral wall thickness measured in short-axis view; (**C**) LV ejection fraction and RV fractional area change; (**D**) mitral and tricuspid E/A wave velocity ratios measured in four-chamber view. Two-way ANOVA tests with Sidak correction: adjusted *P*-values (*) <0.05, (**) <0.01 and (***) <0.001 for comparing sham vs PN at each time point. D0, baseline; D3: postoperative day 3; D7: postoperative day 7; D28: postoperative day 28; LV: left ventricle; PN: pneumonectomy; RA: right atrium; RV: right ventricle.

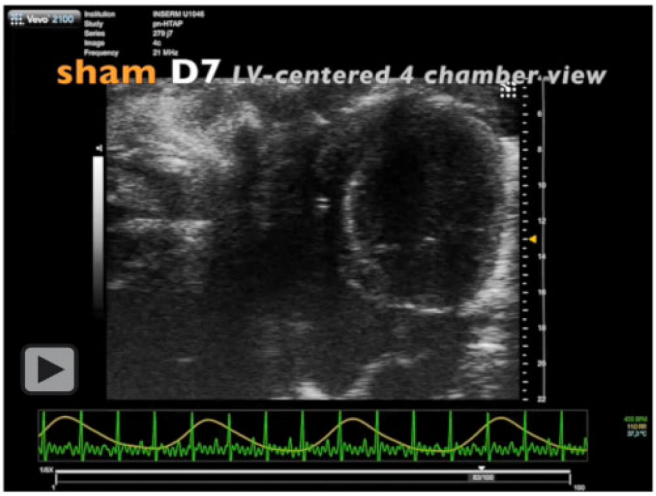

Video 1: Transthoracic echocardiography in a rat from the sham group on postoperative day 7 (four-chamber view, short-axis view and pulmonary artery-centred short-axis view). Acquired with Vevo 2100™ (FUJIFILM VisualSonics®).

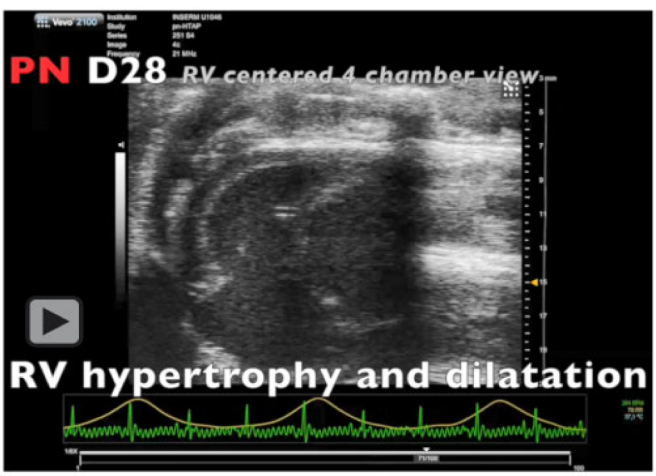

Video 2: Transthoracic echocardiography in rats from the pneumonectomy (PN) group on postoperative days 7 and 28 (four-chamber view, short-axis view and pulmonary artery-centred short-axis view) showing right ventricle dilatation, hypertrophy of the RV lateral wall and a paradoxical septum motion in the PN group. Acquired with Vevo 2100™ (FUJIFILM VisualSonics®).

DISCUSSION

Although lobar and sublobar resections are the treatment of choice for lung cancer, which can better preserve the lung function and minimize the impact on the cardiopulmonary circulation, PN still represents 10–15% of lung resection surgeries. The effects of PN on right heart function have been observed in the clinical setting for many years, contributing to the poor prognosis observed after this type of surgery, associated with high morbidity and an in-hospital mortality of 8% [1]. Most of the previous studies used left PN or relied on multiple-hit methods and agents like monocrotaline [11–16]. It was of major importance to develop a small-animal model of PH after right PN only, which is directly relevant to the scope of thoracic surgery and perioperative medicine.

In our model, a moderate and sustained PH occurred after PN and was associated with a proportional and selective right heart remodelling. Kocatürk *et al.* [13] found almost the same level of systolic PAP 1 month after PN in dogs, with right heart dilatation. Other authors reported a transient PH following left PN in pigs [11], as PAP was normalized 72 h after surgery. In human studies, a gradual increase in PAP is described following PN [3], more severe after right-side resection than left-side resection and associated with progressive RV dilatation [3, 6, 7].

Probably, PH and RV remodelling may depend on both the magnitude of pulmonary resection and the adaptive lung growth capability, which depend on sex and age and are species specific [22, 23]. If there is a resected-volume threshold below which no complications occur, the right-sided PN (∼63% of lung mass in rats) appears to be above it. Le Cras *et al.* [23] highlighted an RV hypertrophy after right PN but no RV alteration after right bilobectomy in rats. The contralateral lung growth and neoangiogenesis after PN could be protective mechanisms by lowering the impact of high blood flow. Future research could study the impact of targeted anti-angiogenic therapies such as anti-VEGF (vascular endothelial growth factor) used in lung cancer on lung growth capabilities after PN.

The RV systolic function was preserved in our model. Previous human studies reported contrasting results. Authors noted that RV ejection fraction was decreased by ∼20% within 3 days after PN, without changes in the cardiac output at rest [7, 24]. Regarding the LV function impairment, a plausible explanation is

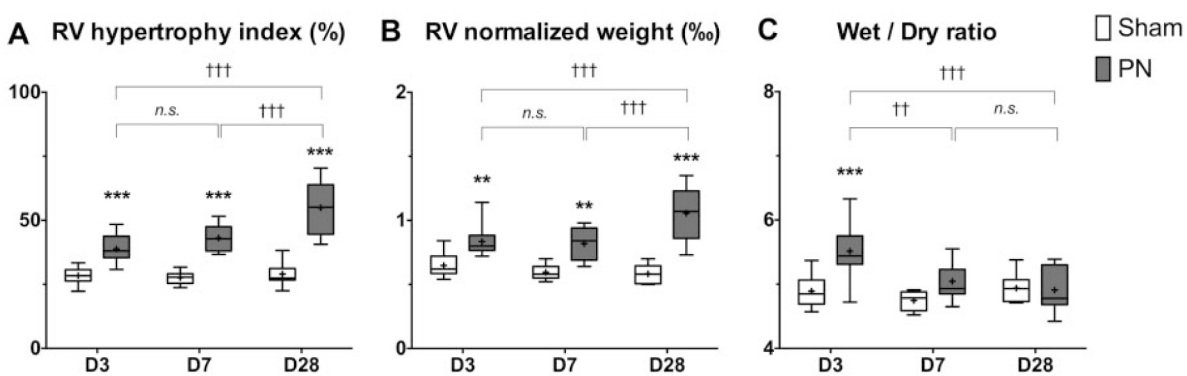

Figure 3: Gravimetric measurements. RV hypertrophy assessed by the right ventricle hypertrophy index [Fulton index = right ventricle/(left ventricle + septum) weight] (**A**) and the RV-normalized weight (RV weight/animal weight) (**B**) and pulmonary oedema estimated by the lung wet/dry ratio (**C**) in the sham and PN groups on D3, D7 and D28 (mean ± SD, median, min to max). Two-way ANOVA tests with Sidak correction: adjusted *P*-values (*) <0.05, (**) <0.01 and (***) <0.001 for comparing sham vs PN at each time point; adjusted *P*-values (†) <0.05, (††) <0.01 and (†††) <0.001 for comparing time effect in each group. D3: postoperative day 3; D7: postoperative day 7; D28: postoperative day 28; RV: right ventricle; PN: pneumonectomy.

that the RV dilatation probably altered the ventricular interdependence leading to LV ejection fraction decrease. Given that ventricles share the same short-termed inextensible pericardium, the RV volume or pressure overloading affects LV function, which is enhanced by a thickened RV-free wall. The displacement of the interventricular septum with paradoxical movement attests that the RV afterload dramatically increased.

In the literature, there is evidence supporting a cardiorespiratory functional deterioration for exercise tolerance, in both the early [24] and late postoperative periods [2]. Authors found deteriorated RV function, elevated PAP and elevated right atrium pressure only during exercise, 3 days after pulmonary resection [24]. Moreover, Miyazawa *et al.* [2] remarkably demonstrated that cardiac output adjustment to exercise was progressively impaired over time and that PAP and vascular resistance increased with increasing exercise load.

In line with the haemodynamic parameters, PH was related to the high muscularization rate of distal pulmonary arteries and a dramatic increase in wall thickness. It is therefore undeniable that PH is a progressive process. Le Cras *et al.* [23] found almost the same rates of muscularized arteries 3 weeks after right PN. Indeed, it is unlikely that PH will regress without a haemodynamic unloading intervention [25]. The pulmonary vascular remodelling was associated with an *in situ* PA-SMC growth and lung inflammation described as a modest infiltration of macrophages, frequently linked to PH.

Our data suggest an early and transitory pulmonary oedema, as the wet/dry ratio was normalized at late stages, which is in line with previous studies in large animals [11, 12]. This is also concordant with other models of increased blood flow, such as aorto-pulmonary shunt, in which pulmonary oedema could occur in case of profound volume overload. The pathophysiological mechanisms of post-PN pulmonary oedema result from an increased permeability of the alveolar capillary barrier, linked to endothelial cell junction alterations, and increased blood flow [26]. Nonetheless, the role of endothelial cells is not limited to permeability regulation.

We recently showed in idiopathic pulmonary arterial hypertension that PA-SMCs have no self-sufficient proliferation capacity [20], highlighting that PA-SMC growth should be regulated by other triggers. The *in vitro* data provide evidence that P-ECs, in response to shear stress, play a key role in the proliferation of PA-SMC in a paracrine fashion. Shear stress probably increased the levels of PDGF-B transcripts by direct activation of shear stress responsive element located on PDGF-B promoter region [27].

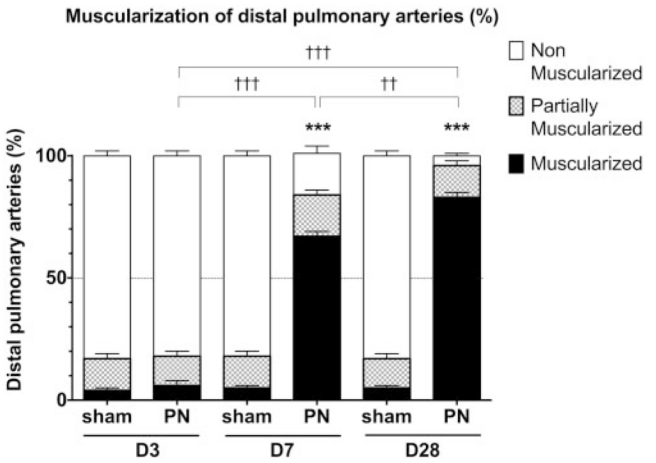

Figure 4: Muscularization of distal pulmonary arteries. Distribution of non-muscularized, partially muscularized and muscularized distal pulmonary arteries in the sham and PN groups on D3, D7 and D28 (percentage ± SD). Two-way ANOVA tests with Sidak correction to compare the proportion of muscularized vessels: adjusted *P*-values (*) <0.05, (**) <0.01 and (***) <0.001 for comparing sham vs PN at each time point; adjusted *P*-values (†) <0.05, (††) <0.01 and (†††) <0.001 for comparing time effect in each group. D3: postoperative day 3; D7: postoperative day 7; D28: postoperative day 28; PN: pneumonectomy.

Limitations

Adding groups of animals treated by lobectomy and left PN could show a dose–effect relationship, which would have strengthened our observation. With the lack of sensors, it remains uncertain if the level of shear stress reproduced *in vitro* is identical to the one following PN in rats. A model of isolated distal

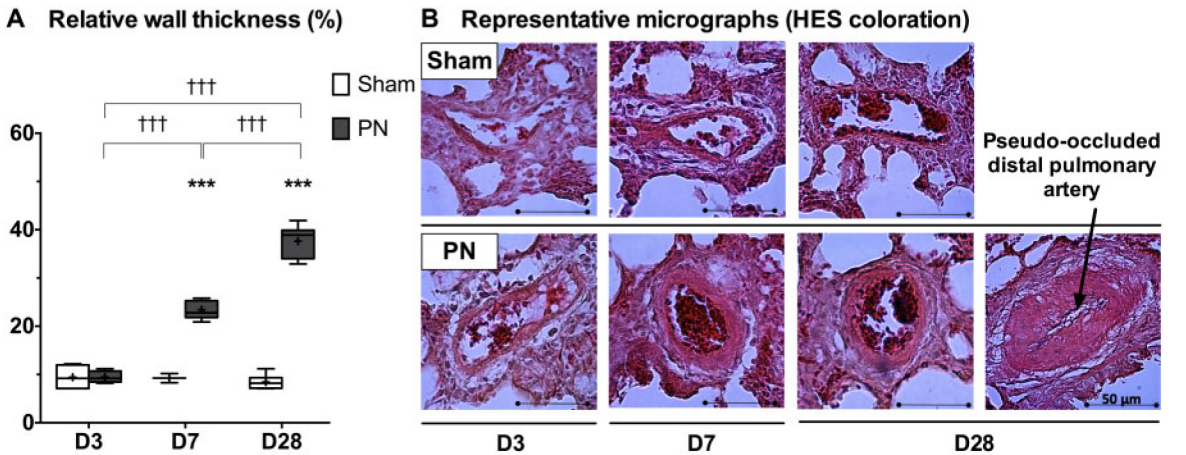

Figure 5: Relative wall thickness of distal pulmonary arteries. Relative wall thickness of distal pulmonary arteries in the sham and PN groups on D3, D7 and D28 (mean ± SD) (**A**). Representative micrographs from HES-stained lung sections of distal pulmonary arteries from sham and PN rats on D3, D7 and D28 (scale bar indicates 50 µm) (**B**). Two-way ANOVA tests with Sidak correction: adjusted *P*-values (*) <0.05, (**) <0.01 and (***) <0.001 for comparing sham vs PN at each time point; adjusted *P*-values (†) <0.05, (††) <0.01 and (†††) <0.001 for comparing time effect in each group. D3: postoperative day 3; D7: postoperative day 7; D28: postoperative day 28; HES: haematoxylin–eosin–saffron; PN: pneumonectomy.

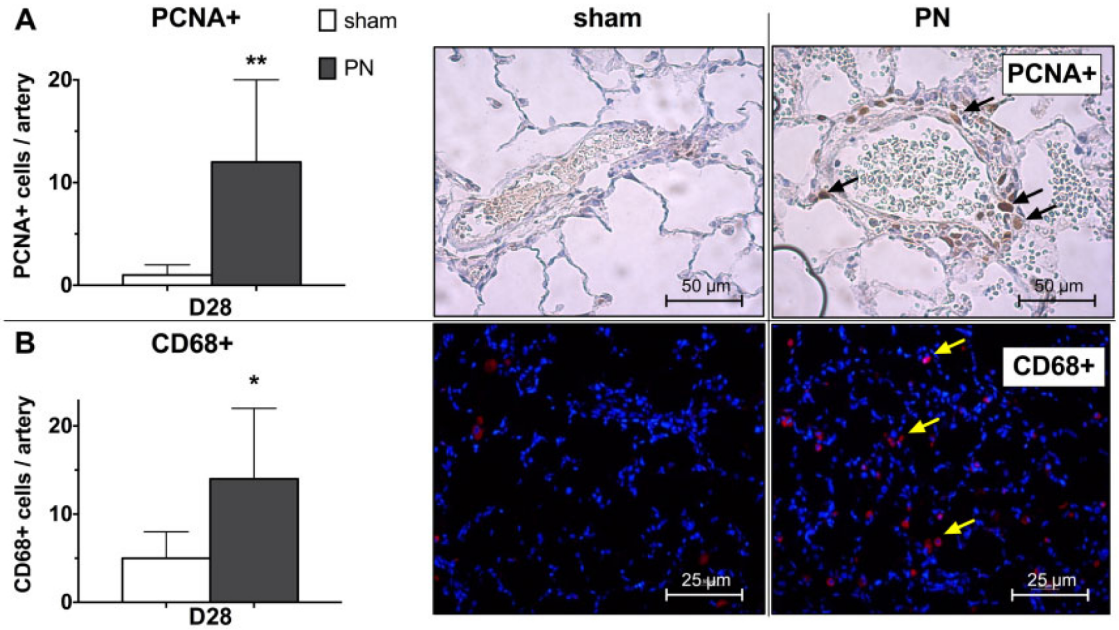

Figure 6: *In situ* PA-SMC proliferation and macrophage infiltrate. Quantification of PA-SMC proliferation (**A**) and macrophage infiltrate (**B**) assessed by PCNA and CD68 immunolabeling, respectively, in the sham and PN groups on D28 (mean ± SD). Representative micrographs showing PCNA+ cells in brown (black arrows, scale bar indicates 50 µm) and CD68+ cells in red (yellow arrows, scale bar indicates 25 µm) in lung sections from rats in the sham and PN groups on D28. Unpaired *t*-tests *P*-values (*) <0.05 and (**) <0.01 for comparing sham vs PN. D28: postoperative day 28; PA-SMC: pulmonary artery smooth muscle cell; PCNA: proliferating cell nuclear antigen; PN: pneumonectomy.

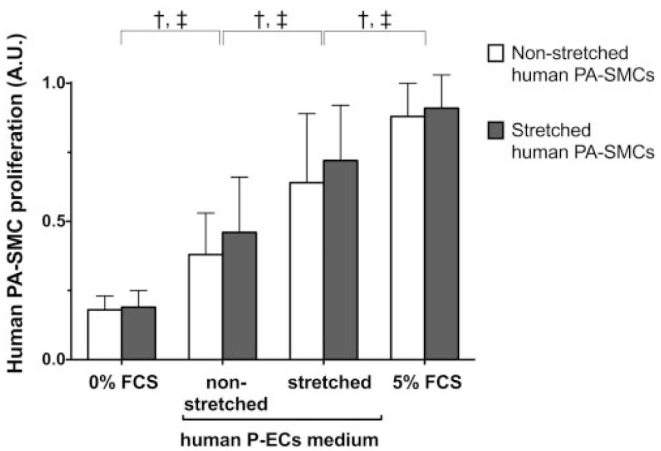

Figure 7: Impact of cyclic stretch on human PA-SMC proliferation. Quantification of human PA-SMC proliferation when exposed (stretched PA-SMCs, grey bars) or not (non-stretched PA-SMCs, white bars) to a 24-h pathological cyclic stretch stimulation, cultured in 4 media: in serum-free media derived from cultured P-ECs previously exposed (stretched P-ECs) or not (non-stretched P-ECs) to a pathological cyclic stretch over 24 h, and in control media (0% or 5% FCS, respectively, minimal and maximal proliferation) (A.U., mean ± SD, 10 samples). Two-way ANOVA tests with Sidak correction. The 2 factors were the medium condition and stretched status of PA-SMCs. Adjusted *P*-value (*) <0.05 for comparing stretched vs non-stretched PA-SMC proliferation in each medium condition; (†) $P < 0.05$ for comparing non-stretched PA-SMC proliferation in different media; (‡) $P < 0.05$ for comparing stretched PA-SMC proliferation in different media. A.U.: arbitrary unit; FCS: foetal calf serum; PA-SMC: pulmonary artery smooth muscle cell; P-EC: pulmonary endothelial cell.

pulmonary artery exposed to different levels of flow rate or elongation would probably have helped to determine a cut-off. Furthermore, response to increased flow must depend on distension and recruitment capabilities of the remaining pulmonary vascular bed, which could be variable from 1 patient to another. Finally, there could be other stressors non-flow related, such as mediastinal shift [28], extracellular matrix alterations, other cell types in the lung environment and other growth factors contributing to vascular remodelling after PN. Pulmonary vasodilators or anti-remodelling drugs, such as PDGF inhibitor, should lower both PAP and RV remodelling after PN.

CONCLUSIONS

Our study provides a comprehensive overview of the pathophysiology and kinetics of PH and heart remodelling over the first month after right PN in rats. Taken together, the results of the animal model in combination with the findings in human cells *in vitro* are an asset to better understand both the pathophysiological and cellular alterations in PH development following PN. Our model is a practical one to study new flow-related pathways and targeted drugs, such as growth factor inhibitors, which is of translational value in patients with flow-induced PH, such as patients with congenital cardiac shunt or patients undergoing large pulmonary resection surgeries.

ACKNOWLEDGEMENTS

The authors thank the small-animal imaging platform of Montpellier (IPAM, Imagerie du Petit Animal de Montpellier,

INSERM U1046, Montpellier, France) for giving us access to the small-animal high-resolution echocardiography; the Department of Thoracic Surgery of the Marie-Lannelongue Hospital (Département de Chirurgie Thoracique, Hôpital Marie Lannelongue, Le Plessis-Robinson, France) and the French National Reference Center for Pulmonary Vascular Diseases (Centre National de Référence des maladies vasculaires pulmonaires, Le Kremlin-Bicêtre, France) for providing the lung specimens and human cells; Jean-Philippe Berthet (Department of Thoracic Surgery, Pasteur Hospital, Nice, France), Joanna Arthur-Ataam and Azzouz Charrabi (PhyMedExp Laboratory, Montpellier, France) for their help and support in experiments; and Claire Duflos (Biostatistics Department, Montpellier University Hospital, Montpellier, France) for her help in statistical analysis and interpretation.

Funding

Support for this study was received solely from institutional and/or departmental sources. There are no sponsors, no grants and no relationships with industry.

Conflict of interest: none declared.

Author contributions

Pierre Sentenac: Conceptualization; Data curation; Formal analysis; Investigation; Methodology; Software; Writing—original draft; Writing—review & editing. **Gianluca Samarani:** Conceptualization; Formal analysis; Investigation; Methodology; Supervision; Validation; Writing—review & editing. **Patrice Bideaux:** Conceptualization; Formal analysis; Investigation; Methodology; Validation; Writing—review & editing. **Pierre Sicard:** Investigation; Methodology; Resources; Software; Validation; Writing—review & editing. **Benjamin Bourdois:** Data curation; Formal analysis; Investigation; Software; Validation; Visualization; Writing—review & editing. **Sylvain Richard:** Conceptualization; Formal analysis; Methodology; Project administration; Resources; Supervision; Validation; Writing—review & editing. **Pascal H. Colson:** Conceptualization; Formal analysis; Methodology; Project administration; Resources; Supervision; Validation; Writing—review & editing. **Saadia Eddahibi:** Conceptualization; Data curation; Formal analysis; Investigation; Methodology; Project administration; Resources; Software; Supervision; Validation; Visualization; Writing—review & editing.

Reviewer information

European Journal of Cardio-Thoracic Surgery thanks the anonymous reviewers for their contribution to the peer review process of this article.

REFERENCES

[1] Thomas PA, Berbis J, Baste J-M, Le Pimpec-Barthes F, Tronc F, Falcoz P-E *et al.* Pneumonectomy for lung cancer: contemporary national early morbidity and mortality outcomes. J Thorac Cardiovasc Surg 2015;149:73–82.

[2] Miyazawa M, Haniuda M, Nishimura H, Kubo K, Amano J. Longterm effects of pulmonary resection on cardiopulmonary function. J Am Coll Surg 1999;189:26–33.

[3] Foroulis CN, Kotoulas CS, Kakouros S, Evangelatos G, Chassapis C, Konstantinou M *et al.* Study on the late effect of pneumonectomy on right heart pressures using Doppler echocardiography. Eur J Cardiothorac Surg 2004;26:508–14.

[4] Potaris K, Athanasiou A, Konstantinou M, Zaglavira P, Theodoridis D, Syrigos KN. Pulmonary hypertension after pneumonectomy for lung cancer. Asian Cardiovasc Thorac Ann 2014;22:1072–9.

[5] Lugg ST, Agostini PJ, Tikka T, Kerr A, Adams K, Bishay E *et al.* Long-term impact of developing a postoperative pulmonary complication after lung surgery. Thorax 2016;71:171–6.

[6] Venuta F, Sciomer S, Andreetti C, Anile M, Giacomo TD, Rolla M *et al.* Long-term Doppler echocardiographic evaluation of the right heart after major lung resections. Eur J Cardiothorac Surg 2007;32:787–90.

[7] Kowalewski J, Brocki M, Dryjanski T, Kapron K, Barcikowski S. Right ventricular morphology and function after pulmonary resection. Eur J Cardiothorac Surg 1999;15:444–8.

[8] Amar D, Roistacher N, Burt M, Reinsel RA, Ginsberg RJ, Wilson RS. Clinical and echocardiographic correlates of symptomatic tachydysrhythmias after noncardiac thoracic surgery. Chest 1995;108:349–54.

[9] Turnage WS, Lunn JJ. Postpneumonectomy pulmonary edema: a retrospective analysis of associated variables. Chest 1993;103:1646–50.

[10] Simonneau G, Montani D, Celermajer DS, Denton CP, Gatzoulis MA, Krowka M *et al.* Haemodynamic definitions and updated clinical classification of pulmonary hypertension. Eur Respir J 2019;53:1801913.

[11] Berthet J-P, Attard O, Solovei L, Bourdin A, Serre I, Molinari N *et al.* Delayed pulmonary arterial hypertension in relation to pulmonary damage score after pneumonectomy under protective ventilation: experimental study. Eur Surg Res 2013;51:172–80.

[12] Kuzkov VV, Suborov EV, Kirov MY, Kuklin VN, Sobhkhez M, Johnsen S *et al.* Extravascular lung water after pneumonectomy and one-lung ventilation in sheep. Crit Care Med 2007;35:1550–9.

[13] Kocatürk M, Salci H, Yilmaz Z, Bayram AS, Koch J. Pre- and postoperative cardiac evaluation of dogs undergoing lobectomy and pneumonectomy. J Vet Sci 2010;11:257–64.

[14] White RJ, Meoli DF, Swarthout RF, Kallop DY, Galaria II, Harvey JL *et al.* Plexiform-like lesions and increased tissue factor expression in a rat model of severe pulmonary arterial hypertension. Am J Physiol Lung Cell Mol Physiol 2007;293:L583–90.

[15] Dorfmüller P, Chaumais M-C, Giannakouli M, Durand-Gasselin I, Raymond N, Fadel E *et al.* Increased oxidative stress and severe arterial remodeling induced by permanent high-flow challenge in experimental pulmonary hypertension. Respir Res 2011;12:119.

[16] Happé CM, de Raaf MA, Rol N, Schalij I, Vonk-Noordegraaf A, Westerhof N *et al.* Pneumonectomy combined with SU5416 induces severe pulmonary hypertension in rats. Am J Physiol Lung Cell Mol Physiol 2016;310:L1088–1097.

[17] Dickinson MG, Bartelds B, Borgdorff MAJ, Berger R. The role of disturbed blood flow in the development of pulmonary arterial hypertension: lessons from preclinical animal models. Am J Physiol Lung Cell Mol Physiol 2013;305:L1–14.

[18] Eddahibi S, Guignabert C, Barlier-Mur A-M, Dewachter L, Fadel E, Dartevelle P *et al.* Cross talk between endothelial and smooth muscle cells in pulmonary hypertension: critical role for serotonin-induced smooth muscle hyperplasia. Circulation 2006;113:1857–64.

[19] Eddahibi S, Raffestin B, Clozel M, Levame M, Adnot S. Protection from pulmonary hypertension with an orally active endothelin receptor antagonist in hypoxic rats. Am J Physiol Heart Circ Physiol 1995;268:H828–35.

[20] Perros F, Sentenac P, Boulate D, Manaud G, Kotsimbos T, Lecerf F *et al.* Smooth muscle phenotype in idiopathic pulmonary hypertension: hyper-proliferative but not cancerous. Int J Mol Sci 2019;20:3575.

[21] Birukov KG, Jacobson JR, Flores AA, Ye SQ, Birukova AA, Verin AD *et al.* Magnitude-dependent regulation of pulmonary endothelial cell barrier function by cyclic stretch. Am J Physiol Lung Cell Mol Physiol 2003;285:L785–97.

[22] Almeida FM, Saraiva-Romanholo BM, Vieira RP, Moriya HT, Ligeiro-de-Oliveira AP, Lopes FD *et al.* Compensatory lung growth after bilobectomy in emphysematous rats. PLoS One 2017;12:e0181819.

[23] Le Cras TD, Fernandez LG, Pastura PA, Laubach VE. Vascular growth and remodeling in compensatory lung growth following right lobectomy. J Appl Physiol 2005;98:1140–8.

[24] Okada M, Ota T, Okada M, Matsuda H, Okada K, Ishii N. Right ventricular dysfunction after major pulmonary resection. J Thorac Cardiovasc Surg 1994;108:503–11.

[25] Mercier O, Sage E, de Perrot M, Tu L, Marcos E, Decante B *et al.* Regression of flow-induced pulmonary arterial vasculopathy after flow correction in piglets. J Thorac Cardiovasc Surg 2009;137:1538–46.

[26] Lohser J, Slinger P. Lung injury after one-lung ventilation: a review of the pathophysiologic mechanisms affecting the ventilated and the collapsed lung. Anesth Analg 2015;121:302–18.

[27] Resnick N, Collins T, Atkinson W, Bonthron DT, Dewey CF, Gimbrone MA. Platelet-derived growth factor B chain promoter contains a cis-acting fluid shear-stress-responsive element. Proc Natl Acad Sci USA 1993;90:4591–5.

[28] Stavroulias D, Ampollini L, Carbognani P, Rusca M. Post-pneumonectomy cavity: is there still a cavity?. Ann Thorac Surg 2010;89:312 10.1016/j.athoracsur.2009.02.086